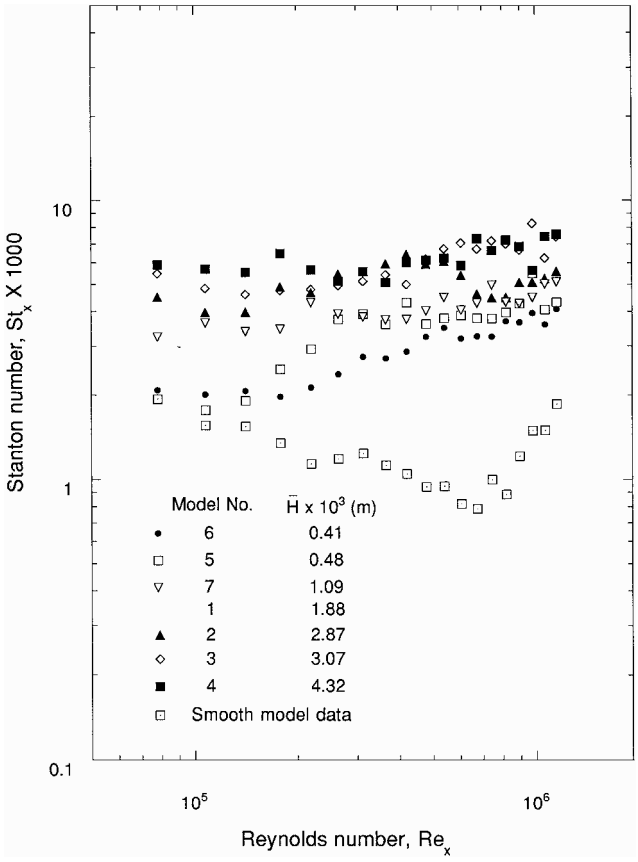

Fig. 3 Stanton number vs Reynolds number: comparison of the roughness models at u_∞ = 32.6 m/s and θ = 41 deg.

approximately $Re_x = 1.2 \times 10^5$ and are fully turbulent at approximately $Re_x = 3.5 \times 10^5$.

Figure 3 is for the high-acceleration case of 41 deg with a Reynolds number again based on the freestream velocity and local axial position. The data for roughness model 1 at this angle was lost in the processing phase. The behavior of the remaining models is similar to Fig. 2, with the Stanton numbers increasing with increasing $\bar{H}$ up to $Re_x = 2.4 \times 10^5$ and with an overlapping in the data for models 2–4 occurring for higher Reynolds numbers. The Stanton numbers are higher than in Fig. 2, and there is a wider spacing between the curves. Transition begins for models 5 and 6 at approximately $Re_x = 2.0 \times 10^5$ (a delay from the case in Fig. 2), and there is no apparent evolution toward an asymptotic state as the Stanton numbers continue to increase.

A complete set of the smooth and rough model data for the accelerated cases are available in the work by Dukhan.[6]

Conclusions

Stanton number results were obtained for the rate of convective heat transfer from aluminum castings of ice-roughened surfaces in accelerated flow. Seven models representing different types of ice accretions were tested in a wind tunnel for free-stream velocities of 9.4, 20.7, and 32.6 m/s and at inclination angles of 5, 14, 23, and 41 deg. For the smooth model, acceleration angle in general lowered the heat transfer rate before transition and delayed the onset of transition as compared to the 0-deg case. For the roughened models, the heat transfer rates for Reynolds numbers up to $Re_x = 2.4 \times 10^5$ were proportional to the roughness element height of the model, after which overlapping occurred in the data for the higher roughness element models. This was behavior similar to the parallel flow data in Ref. 1.

Acknowledgment

This effort was funded under Grant NAG 3-72 by the NASA John H. Glenn Research Center at Lewis Field, Cleveland, Ohio.

References

[1]Dukhan, N., Masiulaniec, K. C., De Witt, K. J., and Van Fossen, G. J., "Experimental Heat Transfer Coefficients from Ice-Roughened Surfaces for Aircraft Deicing Design," *Journal of Aircraft* (to be published).

[2]Hosni, M. H., Coleman, H. W., and Taylor, R. P., "Measurement and Calculations of Rough Wall Heat Transfer in the Turbulent Boundary Layer," *International Journal of Heat and Mass Transfer*, Vol. 34, No. 4, 1991, pp. 1067–1082.

[3]Hosni, M. H., Coleman, H. W., and Garner, J. W., "Roughness Shape Effect on Heat Transfer and Skin Friction in Rough-Wall Turbulent Boundary Layer," *International Journal of Heat and Mass Transfer*, Vol. 36, No. 1, 1993, pp. 147–153.

[4]Coleman, H. W., "Momentum and Energy Transport in the Accelerated Fully Rough Turbulent Boundary Layer," Ph.D. Dissertation, Dept. of Mechanical Engineering, Stanford Univ., Stanford, CA, March 1976.

[5]Poinsatte, P. E., Van Fossen, G. J., and De Witt, K. J., "Roughness Effect on Heat Transfer from a NACA 0012 Airfoil," *Journal of Aircraft*, Vol. 28, No. 12, 1991, pp. 908–911.

[6]Dukhan, N., "Measurements of the Convective Heat Transfer Coefficient from Ice Roughened Surfaces in Parallel and Accelerated Flows," Ph.D. Dissertation, Dept. of Mechanical, Industrial and Manufacturing Engineering, Univ. of Toledo, Toledo, OH, Dec. 1996.

[7]Keller, F. J., "Flow and Thermal Structure in Heated Transitional Boundary Layers with and Without Stream-Wise Acceleration," Ph.D. Dissertation, Clemson Univ., Clemson, SC, Aug. 1993.

[8]Schlichting, H., *Boundary-Layer Theory,* 7th ed., McGraw–Hill, New York, 1987, pp. 489–496.

[9]Kays, W. M., *Convective Heat and Mass Transfer,* McGraw–Hill, New York, 1966, pp. 214–226.

Unified Model Deformation and Flow Transition Measurements

Alpheus W. Burner*
NASA Langley Research Center,
Hampton, Virginia 23681-2199
Tianshu Liu† and Sanjay Garg†
High Technology Corporation, Hampton, Virginia 23666
and
James H. Bell‡ and Daniel G. Morgan‡
NASA Ames Research Center,
Moffett Field, California 94035-1000

Introduction

THE number of optical techniques that may potentially be used during a given wind-tunnel test is continually growing. These include parameter sensitive paints that are sensitive to temperature or pressure, several different types of off-body and on-body flow visualization techniques, optical angle of attack (AOA), optical measurement of model deformation, optical techniques for determining density or velocity, and spectroscopic techniques for determining various flowfield parameters. Often in the past the various optical techniques were developed independently of each other, with little or no consideration for other techniques that might also be used during a given test. Part of the justification for this approach was that

Received 12 June 1999; accepted for publication 21 July 1999.

*Research Scientist, MS 236. Senior Member AIAA.
†Research Scientist, 28 Research Drive. Member AIAA.
‡Aerospace Engineer. Member AIAA.

many of the measurement attempts with optical techniques were for demonstration or proof-of-concept purposes rather than for routine measurements.[1] In order not to compromise wind-tunnel productivity, the techniques selected for a given test should ideally work together in a seamless and unified manner so as not to require separate run series. However, unified instrumentation does not necessarily mean that common cameras or data acquisition systems are employed for the various techniques. Such attempts at creating a hybrid measurement system often result in an awkward system that is not well suited for practical use. Rather, what is meant by unification is a cooperative interaction where all needed measurements are obtained without appreciable interference between the techniques.

In addition to concerns about productivity, there are only a limited number of viewing and lighting window ports that must be shared by the various optical techniques in a production wind tunnel. Perhaps even more crucial are conflicting requirements for the various techniques. For example, one technique may require that the test section lights be turned off, interfering with model surveillance, whereas other techniques may require that the test section lights be turned on. It is expected that the issues of unified instrumentation will become increasingly important in the future due to the major emphasis on productivity and the demand for the use of various optical techniques during production testing.

Recently two optical techniques have been increasingly requested for production measurements in NASA wind tunnels. These are the video photogrammetric (or videogrammetric) technique[2] for measuring model deformation, known as the video model deformation (VMD) technique, and the parameter sensitive paints[3,4] for making global pressure and temperature measurements. Considerations for and initial attempts at simultaneous measurements with the pressure sensitive paint (PSP) and the videogrammetric techniques are described in Ref. 5. Temperature sensitive paint (TSP) has been found to be useful for boundary-layer transition detection[3,4] inasmuch as turbulent boundary layers convect heat at higher rates than laminar boundary layers of comparable thickness. Transition is marked by a characteristic surface temperature change wherever there is a difference between model and flow temperatures. Recently, additional capabilities have been implemented in the target-tracking videogrammetric measurement system described in Ref. 6. These capabilities have permitted practical simultaneous measurements using parameter sensitive paint and VMD measurements that led to the first successful unified test with TSP for transition detection in a large production wind tunnel.

Experimental Setup and Results

The NASA Ames Research Center 12-Ft Pressure Wind Tunnel is a closed circuit facility with testing capabilities of Mach number M from 0 to 0.55, Reynolds number per foot R_e from 0.1 to 15×10^6, stagnation pressure from 2 to 90 psia, and temperature range from 540 to 610°R. A radiator mounted in the upstream diffuser section is capable of cooling the flow at rates up to 5°R/min to enable transition detection with TSP. If uncooled, the tunnel can be heated at rates up to 1.5°R/min. The trapezoidal wing (Trap Wing) semispan model used for this test is a high-lift configuration consisting of slat, main wing, and flap with a semispan of 85.2 in.

Simultaneous transition detection and model deformation measurements were made at M from 0.15 to 0.25 and R_e from 3.5×10^6 to 15×10^6 over an AOA range of −4 to 34 deg. The experimental setup is shown in Fig. 1a. A target-tracking model deformation system was used to acquire and to reduce multiple images per data point to calculate twist and bending due to aerodynamic loads of the main wing and trailing-edge flap.[6] The working principles of this system are based on digital photogrammetry. The system consists of a video charge-coupled device (CCD) camera, a computer with a frame grabber, light sources, and specially distributed targets on a model. Software includes image acquisition, target-tracking/centroid calculation, camera calibration, and data processing. Laboratory experiments indicate that the deformation system can achieve an accuracy of 0.001 in. in displacement and 0.005 deg in angle. For this wind-tunnel test, in which a short focal length lens is used to accommodate the large range of AOA, the uncertainties of the bending for the main wing and flap are estimated to be 0.01 and 0.02 in., respectively. The uncertainties of the angle measurements are estimated to be 0.05 and 0.1 deg for the main wing and flap, respectively.

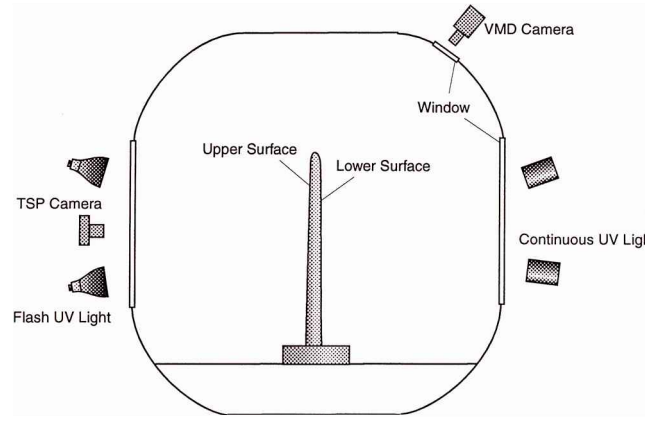

Fig. 1a Schematic of setup looking downstream.

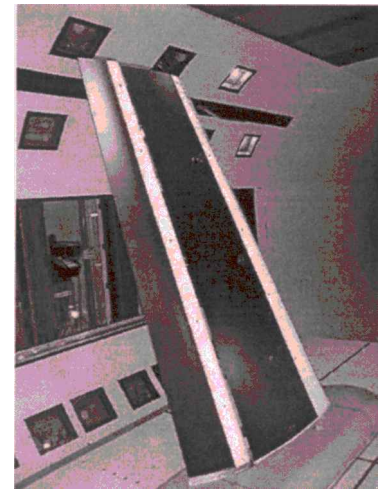

Fig. 1b Upper surface of trap wing showing TSP for transition detection on main wing and flap.

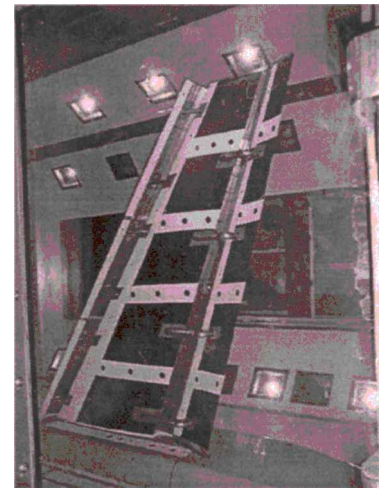

Fig. 1c Lower surface of wing showing black VMD targets on main wing and flap.

The transition detection system consisted of TSP on the upper wing surface, three scientific-grade cooled CCD cameras, several flash UV lights for illumination, and a computer for data processing. Europium Thenoyltrifluoroacetonate (EuTTA) in model airplane dope was used as the TSP. This paint, described more fully in Ref. 4, has a temperature sensitivity of −3.9%/°C. The EuTTA–dope paint was coated on white paint stripes along the main wing, slat,

and trailing-edge flap of the upper wing surface (Fig. 1b). The white basecoat was used to enhance surface scattering and to increase the luminescence emission of the TSP. TSP was applied only on the slat and on the first 20% of chord on the main wing and flap because previous testing of this model in the NASA Langley Research Center 14 × 22 ft tunnel had shown that transition would always occur upstream of these locations. The remainder of the model was painted black as a background for fluorescent minitufts. The flash system, consisting of four 2000-J photographic strobes, was used to illuminate both the TSP and the minitufts. The precision of the light intensity measurements with the cameras was shot-noise limited to 0.5% of full scale, implying a temperature measurement precision of 0.15°C. Because transition measurements depend on relative temperature variation, no attempt was made to determine the absolute accuracy of the temperature measurements.

The deformation measurement system was adapted to work with UV lighting. No change in TSP data acquisition was required because the continuous UV directed toward the lower wing surface to illuminate deformation targets did not appreciably affect the TSP images. The lower surface (instead of the upper surface) was chosen for deformation measurements for several reasons. Larger targets (required by the deformation measurement system due to the use of lower spatial resolution CCD video-rate cameras) were not desirable on the upper surface where transition was to be measured in order not to interfere with the minituft flow visualization. In addition, flash UV illumination of the upper surface would have introduced additional synchronization requirements for the deformation measurement system and would have permitted only one image per data point. Hence, deformation data were acquired on the lower surface with continuous UV lights to produce high contrast images to ensure robust target tracking. Black targets were placed on white paint stripes coated with luminescent paint (EuTTA–dope) on both the main wing and the trailing-edge flap of the lower surface (Fig. 1c). Five target rows were placed on the fuselage and at wing semispan locations of 25, 47, 66, and 84%. (Data are not presented for the 84% semispan row because that row was not always in the field of view over the large AOA range for this test.) A progressive scan CCD camera was used to enable the selection of a relatively long (0.5 s) integration time for continuous UV illumination and a relatively short (0.05 s) integration time for normal test section lighting when TSP data were not to be taken. The model deformation measurement system could also be quickly configured through software changes to take data either simultaneously with TSP using UV illumination or without TSP using normal test section lighting.

TSP data were obtained with three cameras viewing the slat, flap, and wingtip of the model. Because TSP brightness varies with illumination intensity, paint thickness, and temperature, raw TSP images were corrected by ratioing each image with a reference image. The following data acquisition procedure was used: The tunnel was first run for an extended period, without cooling, to raise the temperature of the flow and the model. Reference images were taken of the hot model at several different pitch angles. The cooling system was then activated, and run images were taken over the same AOA sequence while the flow cooled. The cooling sequence generally required 2–3 min, during which time the flow temperature

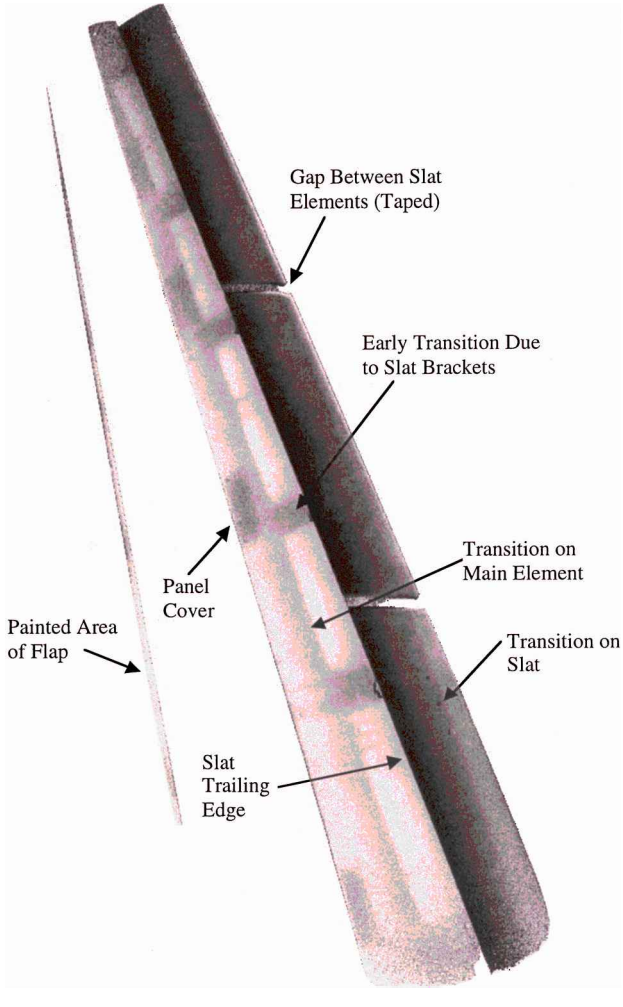

Fig. 2 Transition on the upper surface of the trap wing.

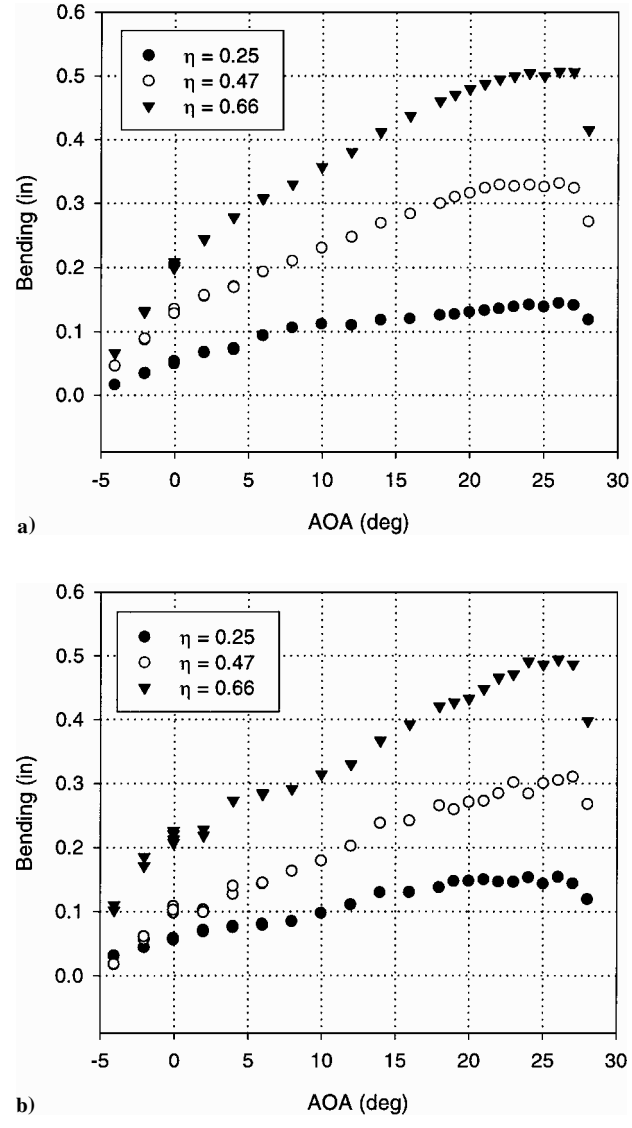

Fig. 3 Wing bending as a function of AOA at three spanwise locations η for a) main wing and b) flap.

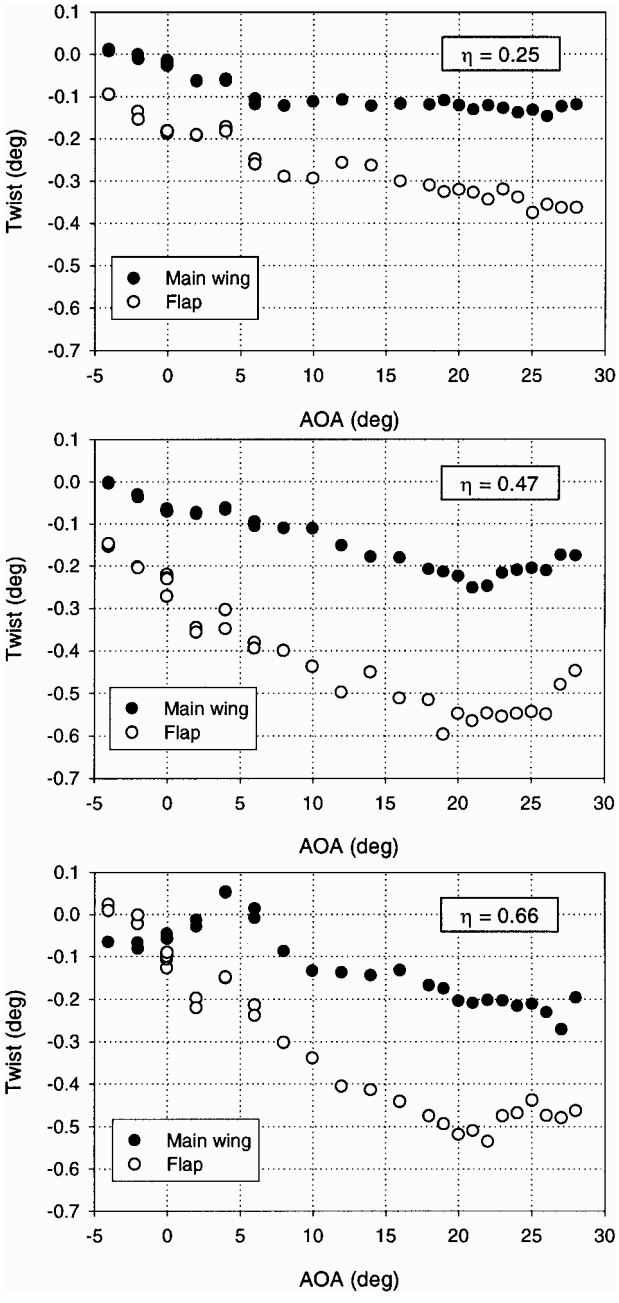

Fig. 4 Wing twist as a function of AOA at three spanwise locations η for main wing and flap.

dropped at about 5°R/min. Internal model temperatures, measured with thermocouples, lagged the flow by from 2°R (slat) to 10°R (main wing).

Figure 2 shows a typical transition image of the slat and main wing of the trap wing captured simultaneously with the deformation data acquisition. The model is at AOA = 24 deg, $M = 0.15$, and total pressure $P_t = 1$ atm with the slat and flap in landing configuration. Bright regions in the image are hot relative to dark regions. The slat is dark relative to the main wing because its lower mass allows it to follow more rapidly the drop in flow temperature. Because the flow cools the model, boundary-layer transition is indicated by a sharp decrease in brightness. This effect can be seen clearly on the main wing, where transition occurs at 10–15% chord except behind the turbulent wakes of the slat brackets.

Examples of the twist and bending data for the main wing and flap taken under continuous UV illumination simultaneously with TSP are presented in Figs. 3 and 4. Data are shown as a function of the AOA at three normalized semispan stations η, where targets were located. The test conditions are $M = 0.15$ and $P_t = 4.3$ atm. Data taken at a higher P_t than for Fig. 2 are shown to emphasize deformation for this very rigid model. The twist and bending were computed with a conformal transformation[6] between wind-on and wind-off spatial coordinates. The relative bending between the flap and the main wing is small as expected because the flap is not rooted in the fuselage, but is firmly attached to the main wing via four rigid brackets. The twist of the flap is generally greater than that of the main wing at a given spanwise station. This is probably due to the large deflection angle of the flap (25 deg) relative to the main wing, which effectively increases flap local AOA and, hence, aerodynamic loading.

Considerations for future unification efforts of TSP or PSP with video photogrammetry include the use of continuous UV on the same surface as the flash UV. Investigations are also underway to determine the appropriate manner in which to apply photogrammetry to generate a deformed surface grid for PSP or TSP mapping.[6] In addition, a unified PSP and deformation test is currently scheduled for the NASA Langley Research Center Unitary Plan Wind Tunnel. Plans are underway for the unification of a number of optical techniques that are in demand at the National Transonic Facility at NASA Langley Research Center, including video photogrammetry, fluorescent minitufts, TSP, and focusing schlieren.

Conclusions

For the first time a transition detection system using TSP and a model deformation measurement system have been unified, enabling simultaneous measurements in a large production wind tunnel at the NASA Ames Research Center. Simultaneous transition detection and twist and bending measurements were made on the main wing and trailing-edge flap of a trapezoidal semispan wing at $M = 0.15$ to 0.25, $R_e = 3.5 \times 10^6$ to 15×10^6, over an AOA range of −4 to 34 deg. The two optical measurement systems worked together seamlessly. The deformation measurement system was also configured with a simple software change to acquire data with normal test section lighting when TSP data were not being taken.

Acknowledgments

The trap wing test at the NASA Ames Research Center 12-ft tunnel was conducted under the Advanced Subsonic Technology High Lift Program. The unified instrumentation effort reported here was supported by funding from the Integrated Instrumentation and Testing Systems program. The support of the operations staff at the NASA Ames Research Center 12-Ft Pressure Tunnel and the collaboration with Michael D. Madson, NASA Ames Research Center, and Kenneth M. Jones and Anthony E. Washburn, NASA Langley Research Center, are gratefully acknowledged.

References

[1]Heyes, A. L., and Whitelaw, J. H., "Review of Optical Methods for Fluid Mechanics," *Advanced Aerodynamic Measurement Technology*, CP-601, AGARD, 1997, pp. 1-1–1-17.

[2]Burner, A, W., "Model Deformation Measurements at NASA Langley Research Center," *Advanced Aerodynamic Measurement Technology*, CP-601, AGARD, 1997, pp. 34-1–34-9.

[3]McLachlan, B. G., and Bell, J. H., "Pressure-Sensitive Paint in Aerodynamic Testing," *Experimental Thermal and Fluid Science*, Vol. 10, No. 4, 1995, pp. 470–485.

[4]Liu, T., Campbell, B., Burns, S., and Sullivan, J., "Temperature- and Pressure-Sensitive Paints in Aerodynamics," *Applied Mechanics Reviews*, Vol. 50, No. 4, 1997, pp. 227–246.

[5]Bell, J. H., and Burner, A. W., "Data Fusion in Wind Tunnel Testing: Combined Pressure Paint and Model Deformation Measurements," AIAA Paper 98-2500, June 1998.

[6]Liu, T., Radeztsky, R., Garg, S., and Cattafesta, L., "A Videogrammetric Model Deformation System and Its Integration with Pressure Paint," AIAA Paper 99-0568, Jan. 1999.